IEEE Access
Multidisciplinary | Rapid Review | Open Access Journal

Received July 19, 2021, accepted September 1, 2021, date of publication September 10, 2021, date of current version September 17, 2021.

Digital Object Identifier 10.1109/ACCESS.2021.3111650

RSS-Based Indoor Localization Using Min-Max Algorithm With Area Partition Strategy

KUO YANG, ZHONGHUA LIANG, (Senior Member, IEEE), REN LIU, AND WEI LI, (Member, IEEE)

Department of Communication Engineering, School of Information Engineering, Chang'an University, Xi'an 710064, China

Corresponding author: Zhonghua Liang (lzhxjd@hotmail.com)

This work was supported in part by the Natural Science Basic Research Project in Shanxi Province of China under Grant 2020JM-242 and Grant 2021JM-185, in part by the National Natural Science Foundation of China under Grant 61871314, and in part by the Fundamental Research Funds for the Central Universities, CHD under Grant 300102249303.

ABSTRACT Min-Max algorithm was widely used as a simple received signal strength (RSS-) based algorithm for indoor localization due to its easy implementation. However, the original Min-Max algorithm only achieves coarse estimation in which the target node (TN) is regarded as the geometric centroid of the area of interest determined by measured RSS values. Although extended Min-Max (E-Min-Max) methods using weighted centroid instead of geometric centroid were recently proposed to cope with this problem, the improvement in the localization accuracy is still limited. In this paper, an improved Min-Max algorithm with area partition strategy (Min-Max-APS) is proposed to achieve better localization performance. In the proposed algorithm, the area of interest is first partitioned into four subareas, each of which contains a vertex of the original area of interest. Moreover, a minimum range difference criterion is designed to determine the target affiliated subarea whose vertex is ''closest'' to the target node. Then the target node's location is estimated as the weighted centroid of the target affiliated subarea. Since the target affiliated subarea is smaller than the original area of interest, the weighted centroid of the target affiliated subarea will be more accurate than that of the original area of interest. Simulation results show that the localization error (LE) of the proposed Min-Max-APS algorithm can drop below 0.16 meters, which is less than one-half of that of the E-Min-Max algorithm, and is also less than one-seventh of that of the original Min-Max algorithm. Moreover, for the proposed Min-Max-APS, 90% of the LE are smaller than 0.38 meters, while the same percentage of the LE are as high as 0.49 meters for the E-Min-Max and 1.12 meters for the original Min-Max, respectively.

INDEX TERMS Min-Max algorithm, received signal strength (RSS), area partition, indoor localization, target node (TN).

I. INTRODUCTION

Indoor localization means the process of obtaining locations of one or more indoor devices to determine the position of device users, and therefore indoor localization based services have become an important extension of Global Positioning System (GPS) [1]. Localization accuracy is usually considered as one of the key performances for an indoor localization system. In the past decade, diverse indoor localization techniques were proposed to obtain high localization accuracy [2], [3]. Among them, the received signal strength (RSS-) based localization technique can provide an effective means due to its characteristics of low power and low complexity [4].

The existing RSS-based localization technique can be arguably classified into two types: 1) range-free localization methods and 2) range-based localization methods [5]. In the range-based cases, it is usually assumed that the measured RSS values are available to estimate the distance between the target node (TN) and the anchor nodes (ANs), which can be used to determine the target node's location. As an effective ranging algorithm based on simple geometric considerations, Min-Max algorithm is regarded as one of the most used for RSS-Based localization due to its easy implementation [6].

However, the original Min-Max algorithm only achieves coarse estimation, where the target node's location is

The associate editor coordinating the review of this manuscript and approving it for publication was Moussa Ayyash.

estimated as the geometric centroid of the area of interest determined by measured RSS values [6]–[10]. Although extended Min-Max (E-Min-Max) algorithm [11] and its improved version, referred to as improved E-Min-Max [12], both using weighted centroid instead of geometric centroid, were recently proposed to address this problem, the improvement in the localization accuracy is limited.

In this paper, an improved Min-Max algorithm with area partition strategy (Min-Max-APS) is proposed to achieve better localization performance. In the proposed algorithm, the area of interest is first partitioned into four subareas, each of which contains a vertex of the original area of interest. Moreover, a minimum range difference criterion is designed to determine the target affiliated subarea whose vertex is "closest" to the target node. Then the target node's location is estimated as the weighted centroid of the target affiliated subarea. Because the target affiliated subarea is smaller than the original area of interest, it is expected that the weighted centroid of the target affiliated subarea will be more accurate than that of the original area of interest.

The rest of this paper is organized as follows. In Section II we review the related work including the RSS-based indoor raging model, details about original Min-Max and E-Min-Max algorithms. Then we present the proposed Min-Max-APS algorithm in Section III. Furthermore, simulation results are shown in Section IV, followed by the conclusion in Section V.

II. RELATED WORK

A. RSS-BASED RANGING MODEL

For RSS-based indoor localization, the relationship between distance and path loss can be described as log-normal shadowing model (LNSM) [13], [14]:

$$PL\,(d) = PL\,(d_0) + 10\eta \cdot \log_{10}\left(\frac{d}{d_0}\right) + X_\sigma, \qquad (1)$$

where $PL(d)$ represents the path-loss at a distance d measured in dBm and $PL(d_0)$ is the path-loss at reference distance d_0 (in this paper we assume $d_0 = 1$ meter). η is the path-loss exponent ranging from 2 to 6 in indoor scenarios [15], X_σ denotes the shadow fading which follows zero mean Gaussian distribution with standard deviation σ. The relationship between the RSS and the path-loss at a distance d as:

$$RSS = P_t - PL\,(d)\,, \qquad (2)$$

where P_t is the received signal power in dBm. Substituting (1) into (2), we have:

$$RSS = A - 10\eta \cdot \log_{10}\left(\frac{d}{d_0}\right) - X_\sigma, \qquad (3)$$

where RSS represents the received signal strength in dBm, $A = P_t - PL\,(d_0)$ indicates the RSS value measured at the reference distance d_0.

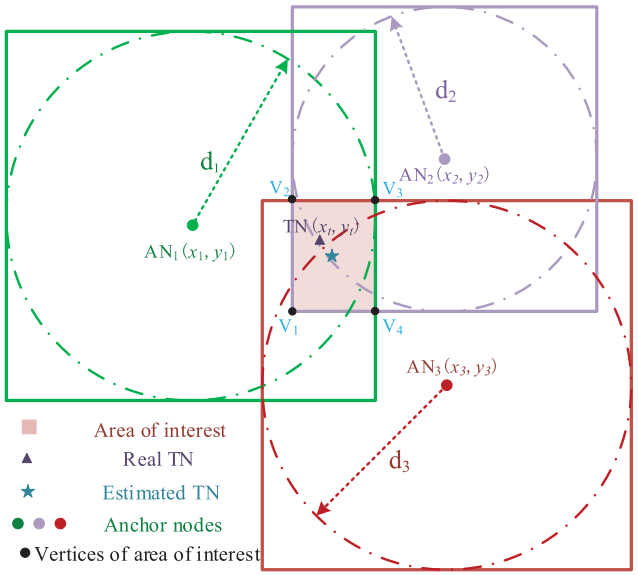

FIGURE 1. Original Min-Max algorithm with three anchor nodes.

B. MIN-MAX ALGORITHM

The original Min-Max algorithm is illustrated in Fig. 1, where N anchor nodes are placed at known locations (x_i, y_i), for $i = 1, 2, \cdots, N$, and a target is located at position (x_t, y_t) which needs to be determined[1]. The RSS values from the ANs are measured by the target node to get relevant distances d_i. Correspondingly, a square (referred to as bounding box in this paper) can be obtained around each AN. Each side of the bounding box is two times the measured distance d_i. These bounding-boxes are used to delimit a region where the position of the TN will be estimated. This region referred to as "area of interest" is a square whose vertices (i.e., V_1, V_2, V_3, V_4) can be obtained as follows [6]:

$$\begin{aligned}
V_1 &= \left[\underbrace{\max\,(x_i - d_i)}_{\triangleq x_{v1}}, \underbrace{\max\,(y_i - d_i)}_{\triangleq y_{v1}}\right], \\
V_2 &= \left[\underbrace{\max\,(x_i - d_i)}_{\triangleq x_{v2}}, \underbrace{\min\,(y_i + d_i)}_{\triangleq y_{v2}}\right], \\
V_3 &= \left[\underbrace{\min\,(x_i + d_i)}_{\triangleq x_{v3}}, \underbrace{\min\,(y_i + d_i)}_{\triangleq y_{v3}}\right], \\
V_4 &= \left[\underbrace{\min\,(x_i + d_i)}_{\triangleq x_{v4}}, \underbrace{\max\,(y_i - d_i)}_{\triangleq y_{v4}}\right], \qquad (4)
\end{aligned}$$

[1]For simplicity, only three anchor nodes are shown in Fig. 1. However, the number of anchor nodes N can be greater than three in practice. For example, in Section IV we let $N = 4$.

where $i = 1, 2, \cdots, N$, and $max(\cdot)$ and $min(\cdot)$ represent the maximum and minimum functions, respectively. In the original Min-Max algorithm, the position of the TN is estimated by calculating the geometric average of the vertices of area of interest as follows [6]:

$$x_t = \frac{\min(x_i + d_i) + \max(x_i - d_i)}{2},$$
$$y_t = \frac{\min(y_i + d_i) + \max(y_i - d_i)}{2}. \quad (5)$$

The original Min-Max localization algorithm is straightforward and easy to implement. In the positioning phase, it only needs a few arithmetic operations, and-that greatly reduce energy consumption and hardware cost. However, due to the impact of multipath fading and noise on the measured RSS values, the original Min-Max algorithm only achieves coarse estimation in which the TN is regarded as the geometric centroid of the area of interest determined by measured noisy RSS values.

C. E-MIN-MAX AND IMPROVED E-MIN-MAX ALGORITHMS

E-Min-Max and improved E-Min-Max algorithms are improved versions of the original Min-Max algorithm, in which a weighted solution instead of the geometric centroid of the original area of interest is used as the target estimation [11], [12]. Four weights W_1, W_2, W_3, and W_4 were first proposed in [11], and two more weights W_5 and W_6 were recently presented in [12]. Since the overall performance of W_4 is the best among the six weights and due to the limited space, in this paper only W_4 is given as follows [11], [12]:

$$W_4(j) = \frac{1}{\sum_{i=1}^{N} \left| D_{i,j}^2 - d_i^2 \right|}, \quad (6)$$

where $D_{i,j}$ represents the Euclidean distance between the anchor node AN_i and the vertex V_j for $j = 1, 2, 3, 4$, as follows:

$$D_{i,j} = \sqrt{(x_i - x_{vj})^2 + (y_i - y_{vj})^2}, \quad (7)$$

where (x_{vj}, y_{vj}) denotes the location of the vertex V_j for $j = 1, 2, 3, 4$, which can be obtained using eq. (4).

The final estimated position is obtained by calculating the weighted centroid as follows [11], [12]:

$$[x_t, y_t] = \left[\frac{\sum_{j=1}^{4} W_4(j) \cdot x_j}{\sum_{j=1}^{4} W_4(j)}, \frac{\sum_{j=1}^{4} W_4(j) \cdot y_j}{\sum_{j=1}^{4} W_4(j)} \right]. \quad (8)$$

E-Min-Max and improved E-Min-Max algorithms determine the area of interest in the same way as the original Min-Max algorithm does. However, in order to improve the localization performance, the position of the TN is estimated as the weighted centroid instead of the geometric centroid of the original area of interest. Although the localization accuracy can be enhanced by using the two improved versions of the original E-Min-Max algorithm, the benefit is still limited.

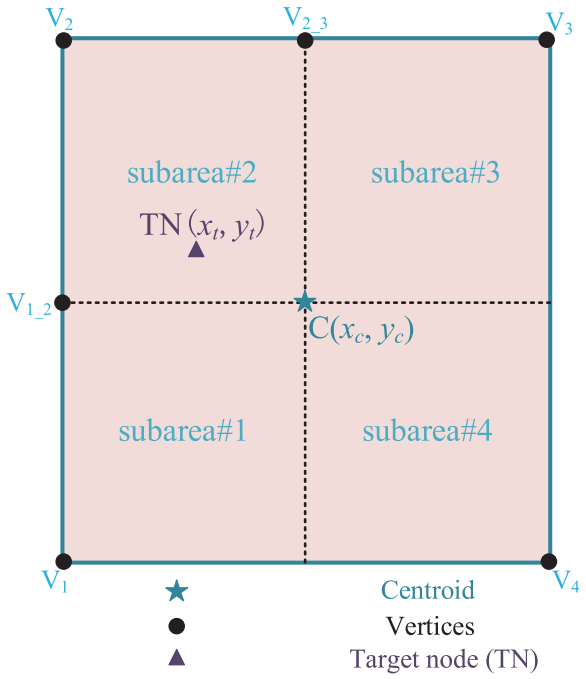

FIGURE 2. Illustration of area partition.

Therefore, in this paper, we try to find a reasonable and efficient way to handle the original area of interest to achieve a better localization performance.

III. PROPOSED MIN-MAX-APS ALGORITHM

The proposed Min-Max-APS algorithm can be implemented via three steps: area partition, determination of target affiliated subarea, and calculation of weighted centroid.

A. AREA PARTITION

As shown in Fig. 2, the original square (area of interest) is divided into four equally sized subareas by the two mid-perpendicular lines. Each subarea contains a vertex of the original square. For simplicity and clarity, the subscript of each vertex is used to indicate the subarea it belongs to. Hence, the four subareas can be represented as *subarea*#1, *subarea*#2, *subarea*#3 and *subarea*#4, respectively. Without loss of generality, we assume the TN is located in *subarea*#2 and the estimated area of interest is reduced to a quarter of the original, the vertices of subarea also changed to V_{1_2}, V_2, V_{2_3} and centroid C. Via area partition, we reduced the final localization area of interest to one-fourth of the original size. Thus, we have eliminated three-quarters of the potential positioning errors points when compared with positioning using the original area of interest.

B. DETERMINATION OF TARGET AFFILIATED SUBAREA

In this subsection, a minimum range difference criterion is designed to determine the target affiliated subarea whose vertex is ''closest'' to the target node. In order to determine the target affiliated subarea, we just need to find which vertex of the original square is ''closest'' to the target node by using

Algorithm 1 Proposed Min-Max-APS Algorithm

Initialization:

1. Locations of anchor nodes AN_i $(i = 1, 2, \cdots, N)$.

Procedure:

1: Calculate the distances d_i $(i = 1, 2, \cdots, N)$ using RSS measurements.
2: Calculate the coordinates of vertices V_j $(j = 1,2, 3, 4)$ and centroid C using (4) and (5) respectively.
3: **for** $i = 1$ **to** $N, j = 1$ **to** 4 **do**
4: Estimate the subscript of the target affiliated subarea $\hat{j}$ using (9) and determine the newly defined area of interest;
5: **end for**
6: **if** $\hat{j}$=1 **then**
7: new vertices=$\{V_1, (V_1 + V_2)/2, C, (V_1 + V_4)/2\}$;
8: **elseif** $\hat{j}$=2 **then**
9: new vertices=$\{(V_1 + V_2)/2, V_2, (V_2 + V_3)/2, C\}$;
10: **elseif** $\hat{j}$=3 **then**
11: new vertices=$\{C, (V_2 + V_3)/2, V_3, (V_3 + V_4)/2\}$;
12: **else** $\hat{j}$=4 **then**
13: new vertices=$\{(V_1 + V_4)/2, C, (V_3 + V_4)/2, V_4\}$;
14: **end if**
15: **for** $j = 1$ **to** 4 **do**
16: Calculate the weights (6) using the new vertices for the newly defined area of interest;
17: **end for**
18: Calculate the estimated location (x_t, y_t) by substituting the weights (6) into (8).

the following criterion:

$$index\ \hat{j} = \underset{\substack{j \\ i=1,2,\cdots,N \\ j=1,2,3,4}}{arg\min} \left| d_i - D_{i,j} \right|, \tag{9}$$

where $\hat{j} \in \{1, 2, 3, 4\}$ denotes the estimated identity of the vertex of the original area of interest which is "closest" to the target node, and $|\cdot|$ represents the absolute value of a scalar parameter. Using geometrical relationship we see that the criterion (9) is based on the fact that the closer the target node is to a vertex V_j, the smaller the range difference $\left| d_i - D_{i,j} \right|$ will be, and at the same time, the more likely the target node is located at the subarea which the vertex V_j belongs to. Therefore, the target affiliated subarea can be effectively estimated using (9).

C. CALCULATION OF WEIGHTED CENTROID

After the target affiliated subarea is determined, it can be regarded as the newly defined area of interest whose vertices will be used to calculate the weighted centroid according to (6)-(8). It is noted that the coordinates of four vertices of the target affiliated subarea are known, or can be easily calculated using geometrical relationship. For example, if *subarea*#2 is determined as the newly defined area of interest whose vertices are V_{1_2}, V_2, V_{2_3}, and C, firstly the coordinates of vertex V_2 are known because vertex V_2 is one of vertices of the original area of interest. Moreover, the coordinates of vertices C, V_{1_2}, and V_{2_3} can be calculated using (4).

Based on the above discussions, the entire procedure of the proposed Min-Max-APS algorithm is given in Algorithm 1.

TABLE 1. Important simulation parameters.

Parameters	Description	Value
η	Path-loss exponent	3
A	RSS value at the reference distance of 1 meter	-35 dBm
σ	Standard deviation of shadow fading	4 dB
N	Number of anchor nodes	4
SNR	Signal-to-noise ratio	0-30 dB

IV. SIMULATIONS RESULTS

An indoor localization scenario based on MATALB simulation platform is designed to evaluate the performance of the proposed Min-Max-APS algorithm. In the simulation, the measured area is regarded as a $20m \times 20m$ square grid with 441 uniformly distributed sampling locations ranging from (0, 0) to (20, 20). For an indoor positioning system, the localization accuracy is usually enhanced when more anchor nodes are utilized in the measured area. Nevertheless, if more actual anchor nodes are deployed, the hardware cost and localization system complexity will be increased [1]. In addition, the placement of four anchor nodes at the four corners of a square area has been widely implemented and tested [12], [16], [17] and it shows good estimation performance of the distance between target and anchor nodes [18]. Therefore, in this paper we only consider the case with $N = 4$, where four ANs are placed at the corners of the measured area, i.e., $AN_1(0, 0)$, $AN_2(0, 20)$, $AN_3(20, 20)$, $AN_4(20, 0)$.

For each signal-to-noise ratio (SNR) value, 200 Monte Carlo trials are conducted to obtain an averaged localization performance. In each trial, a sampling point is selected at random from the measured area as the target location. The localization error (LE) and its cumulative distribution functions (CDFs) are evaluated for the proposed Min-Max-APS algorithm, where the LE is defined as

$$LE = \frac{1}{M} \sum_{m=1}^{M} \|\hat{x}_m - x_m\|_2, \tag{10}$$

where $M = 200$ is the number of Monte Carlo trials, $\hat{x}_m$ and x_m denote the estimated and exact positions of the target node in the m-th Monte Carlo trial, respectively. $\|\hat{x}_m - x_m\|_2$ is the Euclidean distance between $\hat{x}_m$ and x_m. Parameters η and A are set as "3" and "-35dBm" which are typical values for indoor positioning scenarios reported in [15]. Some important simulation parameters are given in Table 1.

First, in Fig. 3 we illustrate the probability distribution of incorrect partitioning at all sampling grids of target locations in the measured area when SNR=15 dB. Moreover, Fig. 4 presents an example of the incorrect partitioning distribution when SNR=15 dB. From Figs. 3 and 4, we see that for our proposed algorithm, there are three potential cases which may result in incorrect partitioning due to the measurement errors in d_i with high probability as follows:

TABLE 2. Comparison of localization error for correct and incorrect partitioning cases at eleven sampled target locations (SNR = 15 dB).

Target position	Correct partitioning		Incorrect partitioning	
	Estimated position	Localization error (m)	Estimated position	Localization error (m)
(0,0)	(0.0107,0.0359)	0.0374	(0.0035,0.0191)	0.0194
(0,10)	(0.0455,9.9213)	0.0909	(0.0454,9.9264)	0.0865
(5,10)	(4.9497,9.4426)	0.5597	(4.9501,10.5693)	0.5714
(10,10)	(10.1272,10.1057)	0.1654	(10.1272,9.8844)	0.1718
(15,10)	(14.9933,9.4447)	0.5553	(14.9931,10.56)	0.5601
(20,10)	(19.7904,9.9816)	0.2104	(19.7904,9.9908)	0.2097
(10,0)	(10.1123,0.2187)	0.2458	(10.0591,0.2184)	0.2262
(10,3)	(10.2325,3.0170)	0.2331	(9.7453,3.0170)	0.2553
(10,17)	(9.7774,16.8637)	0.2610	(10.2423,16.8637)	0.2791
(10,20)	(9.9754,19.9308)	0.0734	(9.9670,19.9307)	0.0767
(20,20)	(19.9836,19.9784)	0.0271	(19.9945,19.9785)	0.0221

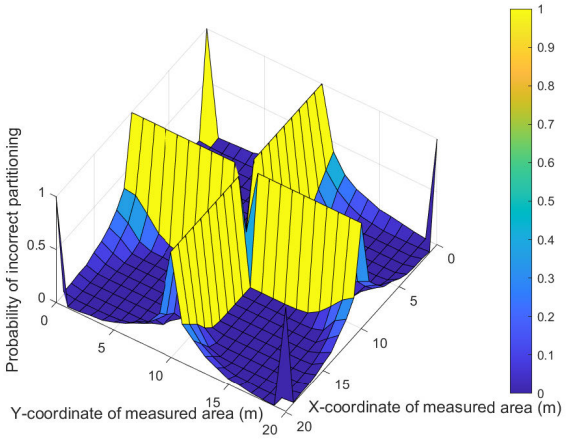

FIGURE 3. Probability distribution of incorrect partitioning at all sampling grids of target locations in the measured area when SNR = 15 dB.

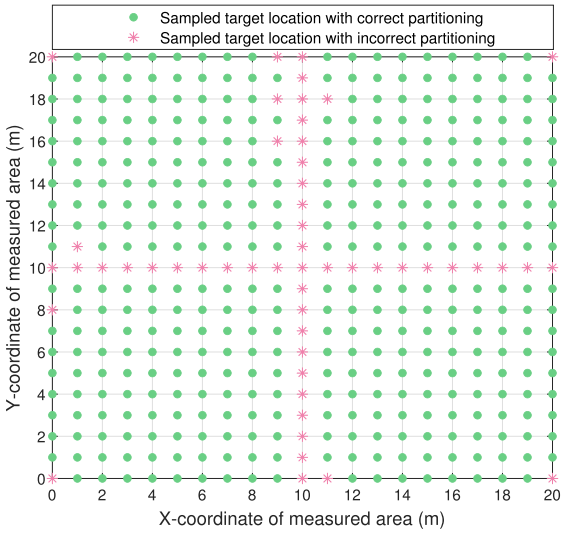

FIGURE 4. An example of incorrect partitioning distribution when SNR = 15 dB.

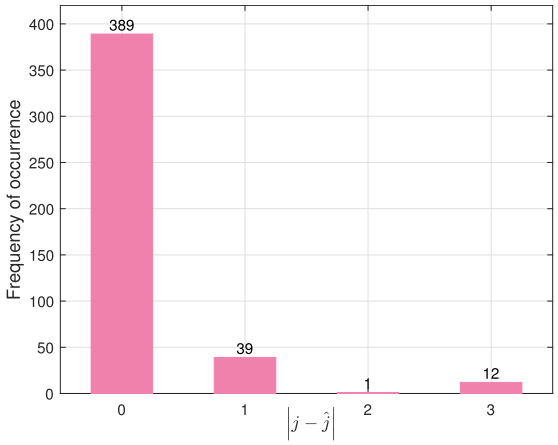

FIGURE 5. Frequency distribution of the difference between the identity of an exact target affiliated subarea j and its estimated index $\hat{j}$, namely $|j-\hat{j}|$ for $j, \hat{j} \in \{1, 2, 3, 4\}$, when SNR = 15 dB.

i) When the target node is close to the horizontal mid-perpendicular line of the measured area, it is most likely that there will be two pairwise d_i measurements with similar value. For example, we have $d_1 \approx d_2$, and the values of D_{11} and D_{22} are also similar. In this case, according to the partitioning criterion (see eq. (9), page 4), it is very likely that an incorrect partitioning will occur between *subarea*#1 and *subarea*#2 due to the measurement errors in d_i. At the same time, we also have $d_3 \approx d_4$, and the values of D_{33} and D_{44} are also similar, and therefore it is highly possible that an incorrect partitioning will happen between *subarea*#3 and *subarea*#4.

ii) Similar to the case of horizontal mid-perpendicular line, when the target node is near the vertical mid-perpendicular line, incorrect partitioning results may be observed between *subarea*#1 and *subarea*#4, and between *subarea*#2 and *subarea*#3, respectively.

iii) Particularly, incorrect partitioning results may be found among the four subareas namely *subarea*#1, *subarea*#2, *subarea*#3, and *subarea*#4, when the target node is adjacent to the centroid of the measured area (intersection of horizontal and vertical mid-perpendicular lines), or the target node is near one of the four corners of the measured area. It is worth mentioning that, when the target node is near any one of the four corners of the measured area, where four anchor nodes AN_i $(i = 1, 2, 3, 4)$ are placed respectively, the measured distance between the target node and the nearest anchor node will be very small, and so will the resulting original area of interest be. Without loss of generality, we assume that the target node is located near the AN_2, we have $d_1 \approx D_{11}$, $d_2 \approx D_{22}$, $d_3 \approx D_{33}$, $d_4 \approx D_{44}$, and

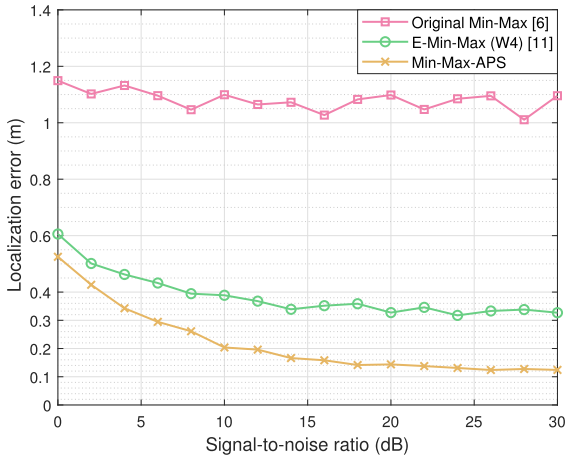

FIGURE 6. Localization error versus signal-to-noise-ratio.

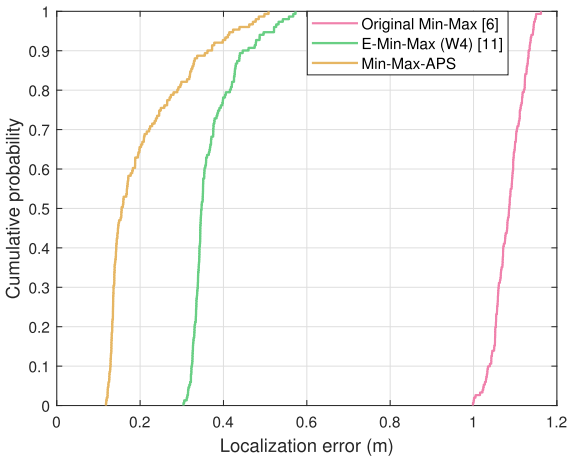

FIGURE 7. Cumulative distribution functions (CDFs) of LE.

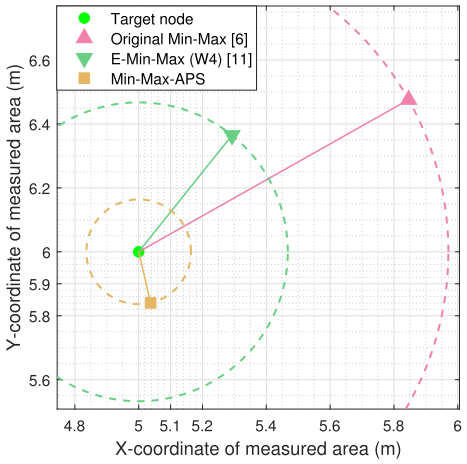

FIGURE 8. Accuracy comparison of the original Min-Max [6], the E-Min-Max [11], and the proposed Min-Max-APS, at a sampling target location (5,6) when SNR = 30 dB.

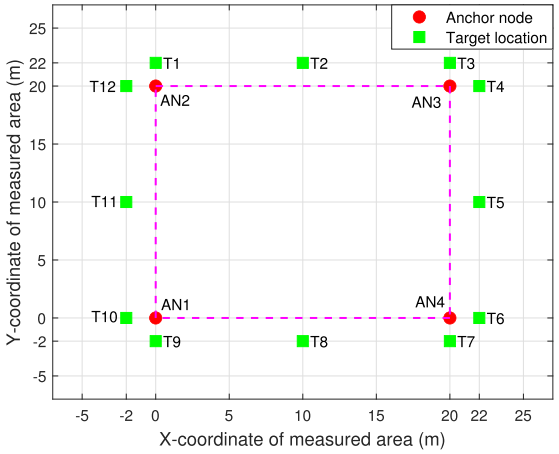

FIGURE 9. Twelve sampled target locations for the case that the target node locates outside the internal zone.

$d_1 \approx d_3$. In this case, according to the partitioning criterion (9), it is very likely that incorrect partitioning will occur among *subarea*#1, *subarea*#2, *subarea*#3 and *subarea*#4. Fortunately, by observing Fig. 1 it can be seen that since d_2 is very small, the resulting original area of interest is also very small. That means the difference of the localization accuracy between correct partitioning and incorrect partitioning will be very small (this can be demonstrated by the results presented in Table 2).

Fig. 5 shows the frequency distribution of the difference between the identity of an exact target affiliated subarea j and its estimated index $\hat{j}$, namely $|j-\hat{j}|$ for $j, \hat{j} \in \{1, 2, 3, 4\}$, when SNR = 15 dB. According to Fig. 2, we see that $|j-\hat{j}|=0$ means the correct partitioning cases, $|j-\hat{j}|=1$ and $|j-\hat{j}|=3$ indicate the incorrect partitioning cases between adjacent subareas (between *subarea*#1 and *subarea*#2, *subarea*#2 and *subarea*#3, *subarea*#3 and *subarea*#4, or between *subarea*#1 and *subarea*#4), and $|j-\hat{j}|=2$ represents the incorrect partitioning cases between diagonal subareas (between *subarea*#1 and *subarea*#3, or between *subarea*#2 and *subarea*#4). From Fig. 5, we see that incorrect partitioning between adjacent subareas acts as a dominant pattern of the partitioning errors.

Table 2 presents the comparison of localization performance for correct and incorrect partitioning cases at eleven sampled target locations when SNR = 15 dB. The eleven target locations are sampled at the horizontal and vertical mid-perpendicular lines and two corners of the measured area, where incorrect partitioning will occur frequently. From Table 2 we see that the difference of the localization accuracy between correct partitioning and incorrect partitioning cases is less than 2.22 cm. Therefore, our proposed algorithm is robust to partitioning errors.

In Fig. 6, the LE performance is presented for the original Min-Max [6], E-Min-Max [11], and the proposed Min-Max-APS algorithms. We see that when the SNR is greater than 15 dB, the LE value of the proposed Min-Max-APS drops below 0.16 meters, which is less than one-half of that of the E-Min-Max [11], and is also less than one-seventh of that of the original Min-Max [6].

Moreover, Fig. 7 shows the CDF profiles of the LE values with SNR ranging from 0 to 30 dB, for the original Min-Max [6], E-Min-Max [11], and the proposed Min-Max-APS algorithms, respectively. We see that for the

TABLE 3. Comparison of localization accuracy for the three investigated algorithms when the target node locates outside the internal area and SNR = 30 dB.

Target position	Original Min-Max [6]		E-Min-Max (W4) [11]		Min-Max-APS	
	Estimated position	Localization error (m)	Estimated position	Localization error (m)	Estimated position	Localization error (m)
T1 = (0,22)	(0.8922,20)	2.1898	(0.1028,21.6428)	0.3717	(0.0608,21.7113)	0.2949
T2 = (10,22)	(9.9983,17.0281)	4.9719	(9.9983,21.5252)	0.4748	(9.9066,21.6479)	0.3642
T3 = (20,22)	(19.1365,20)	2.1784	(9.9715,21.6587)	0.3452	(20.0045,21.7258)	0.2742
T4 = (22,20)	(20,19.0260)	2.2245	(21.8455,19.9258)	0.1714	(21.8663,19.9369)	0.1478
T5 = (22,10)	(17.0287,9.9804)	4.9713	(21.5154,9.9804)	0.4850	(21.6378,9.8955)	0.3770
T6 = (22,0)	(20,0.9193)	2.2011	(21.6525,0.1428)	0.3757	(21.7233,0.0943)	0.2923
T7 = (20,-2)	(19.6619,0.3209)	3.2944	(21.6680,-1.7015)	0.4464	(21.7434,-1.7778)	0.3394
T8 = (10,-2)	(9.9887,2.9887)	4.9876	(9.9887,-1.5471)	0.4530	(9.8785,-1.6627)	0.3585
T9 = (0,-2)	(0.9511,0)	2.2146	(-0.0068,-1.8899)	0.1103	(-0.0121,-1.9027)	0.0980
T10 = (-2,0)	(0.0012,0.9244)	2.2044	(-1.7530,0.0575)	0.2536	(-1.7917,0.0418)	0.2124
T11 = (-2,10)	(2.9901,10.0128)	4.9901	(-1.5340,10.0128)	0.4662	(-1.6506,10.1135)	0.3674
T12 = (-2,20)	(0.1900,19.0578)	2.2108	(-1.5876,19.7490)	0.4827	(-1.6808,19.7972)	0.3781

proposed Min-Max-APS, 90% of the LE values are smaller than 0.38 meters. However, for the E-Min-Max [11] and the original Min-Max [6], the same percentage of the LE values are as high as 0.49 meters and 1.12 meters, respectively.

Finally, in Fig. 8, an accuracy comparison at a sampling target location (5, 6) when SNR = 30 dB is illustrated for the three investigated algorithms to demonstrate the effectiveness of the proposed Min-Max-APS algorithm. It is seen that the target position of the proposed Min-Max-APS algorithm is closest to the real target compared to the original Min-Max [6] and E-Min-Max [11] algorithms.

In this paper, we assume that the anchor nodes are deployed at the four corners of the measured square area and therefore the target node is always inside the internal zone among anchor nodes. This is because for a given localization algorithm, the localization accuracy for the case that the target node locates in the internal zone is usually better than that for the case that the target node locates outside the internal zone. Moreover, we expect that our proposed algorithm will also achieve similar performance gains for the case that the target node locates outside the internal zone. In order to verify our analysis, we evaluated the localization accuracy of the three investigated algorithms for the case that for the case that the target node locates in the internal zone. Fig. 9 shows the twelve sampled target locations for the case that the target node locates outside the internal zone in our simulations. Moreover, Table 3 presents the comparison of localization accuracy for the three investigated algorithms when the target node locates outside the internal area and SNR = 30 dB. We see that at all the twelve sampled target locations, our proposed algorithm still outperforms the original Min-Max [6] and E-Min-Max algorithms [11].

V. CONCLUSION

In this paper, an improved Min-Max algorithm with area partition strategy has been proposed to achieve high-precision localization performance. In the proposed Min-Max-APS algorithm, the original area of interest is first divided into four subareas each of which contains a vertex of the original area of interest. Moreover, a minimum range difference criterion is designed to determine the newly defined area of interest, which can be used to calculate a more accurate weighted centroid. Simulation results show that compared to the original Min-Max [6] and E-Min-Max [11] algorithms, the proposed Min-Max-APS algorithm possesses much more accurate localization performance, and it is the most robust in the whole measured area. Our future research will focus on refining the localization accuracy by iterative implementation of the proposed Min-Max-APS algorithm and optimization of the deployment of anchor nodes.

REFERENCES

[1] F. Zafari, A. Gkelias, and K. K. Leung, "A survey of indoor localization systems and technologies," *IEEE Commun. Surveys Tuts.*, vol. 21, no. 3, pp. 2568–2599, 3rd Quart., 2019.

[2] S. Sadowski and P. Spachos, "RSSI-based indoor localization with the Internet of Things," *IEEE Access*, vol. 6, pp. 30149–30161, 2018.

[3] A. Yassin, Y. Nasser, M. Awad, A. Al-Dubai, R. Liu, C. Yuen, R. Raulefs, and E. Aboutanios, "Recent advances in indoor localization: A survey on theoretical approaches and applications," *IEEE Commun. Surveys Tuts.*, vol. 19, no. 2, pp. 1327–1346, Nov. 2017.

[4] B. Yang, L. Guo, R. Guo, M. Zhao, and T. Zhao, "A novel trilateration algorithm for RSSI-based indoor localization," *IEEE Sensors J.*, vol. 20, no. 14, pp. 8164–8172, Jul. 2020.

[5] B. Yang, Q. Qiu, Q.-L. Han, and F. Yang, "Received signal strength indicator-based indoor localization using distributed set-membership filtering," *IEEE Trans. Cybern.*, early access, Apr. 16, 2020, doi: 10.1109/TCYB.2020.2983544.

[6] E. Goldoni, A. Savioli, M. Risi, and P. Gamba, "Experimental analysis of RSSI-based indoor localization with IEEE 802.15.4," in *Proc. Eur. Wireless Conf. (EW)*, Lucca, Italy, Apr. 2010, pp. 71–77.

[7] B. Rattanalert, W. Jindamaneepon, K. Sengchuai, A. Booranawong, and N. Jindapetch, "Problem investigation of min-max method for RSSI based indoor localization," in *Proc. 12th Int. Conf. Electr. Eng./Electron., Comput., Telecommun. Inf. Technol. (ECTI-CON)*, Jun. 2015, pp. 1–5.

[8] S. Monta, S. Promwong, and V. Kingsakda, "Evaluation of ultra wideband indoor localization with trilateration and min-max techniques," in *Proc. 13th Int. Conf. Electr. Eng./Electron., Comput., Telecommun. Inf. Technol. (ECTI-CON)*, Jul. 2016, pp. 1–4.

[9] Y. Zhao, X. Li, Y. Wang, and C.-Z. Xu, "Biased constrained hybrid Kalman filter for range-based indoor localization," *IEEE Sensors J.*, vol. 18, no. 1, pp. 1647–1655, Feb. 2018.

[10] A. Booranawong, K. Sengchuai, N. Jindapetch, and H. Saito, "An investigation of min-max method problems for RSSI-based indoor localization: Theoretical and experimental studies," *Eng Appl Sci Res*, vol. 47, no. 3, pp. 313–325, Sep. 2020.

[11] J. J. Robles, J. S. Pola, and R. Lehnert, "Extended min-max algorithm for position estimation in sensor networks," in *Proc. IEEE 9th Workshop Positioning Navigat. Commun. (WPNC)*, Mar. 2012, pp. 47–52.

[12] S. Xie, Y. Hu, and Y. Wang, "An improved E-Min-Max localization algorithm in wireless sensor networks," in *Proc. IEEE Intl. Conf. Cons. Electron. (ICCE-China)*, Apr. 2014, pp. 1–4.
[13] S. K. Gharghan, R. Nordin, A. M. Jawad, H. M. Jawad, and M. Ismail, "Adaptive neural fuzzy inference system for accurate localization of wireless sensor network in outdoor and indoor cycling applications," *IEEE Access*, vol. 6, pp. 38475–38489, 2018.
[14] S. K. Gharghan, R. Nordin, and M. Ismail, "Energy efficiency of ultra-low-power bicycle wireless sensor networks based on a combination of power reduction techniques," *J. Sensors*, vol. 2016, pp. 1–21, Jul. 2016.
[15] Y. Zhuang, Y. Li, H. Lan, Z. Syed, and N. El-Sheimy, "Wireless access point localization using nonlinear least squares and multi-level quality control," *IEEE Wireless Commun. Lett.*, vol. 4, no. 6, pp. 693–696, Dec. 2015.
[16] A. Booranawong, K. Sengchuai, N. Jindapetch, and H. Saito, "Enhancement of RSSI-based localization using an extended weighted centroid method with virtual reference node information," *J. Electr. Eng. Technol.*, vol. 15, no. 4, pp. 1879–1897, May 2020.
[17] A. Booranawong, K. Sengchuai, D. Buranapanichkit, N. Jindapetch, and H. Saito, "RSSI-based indoor localization using multi-lateration with zone selection and virtual position-based compensation methods," *IEEE Access*, vol. 9, pp. 46223–46239, 2021.
[18] P. Pivato, L. Palopoli, and D. Petri, "Accuracy of RSS-based centroid localization algorithms in an indoor environment," *IEEE Trans. Instrum. Meas.*, vol. 60, no. 10, pp. 3451–3460, Oct. 2011.

KUO YANG was born in Jining, Shandong, China, in 1995. He is currently pursuing the master's degree with the Department of Communication Engineering, School of Information Engineering, Chang'an University. His research interest includes wireless indoor positioning techniques.

ZHONGHUA LIANG (Senior Member, IEEE) received the B.Sc. degree in radio engineering and the M.Sc. and Ph.D. degrees in information and communication engineering from Xi'an Jiaotong University, Xi'an, China, in 1996, 2002, and 2007, respectively. From July 1996 to August 1999, he was with Guilin Institute of Optical Communications (GIOC), Guilin, China, where he was a System Engineer in optical transmission systems. From 2008 to 2009, he was a Postdoctoral Fellow with the Department of Electrical and Computer Engineering, University of Victoria, Victoria, BC, Canada. Since 2010, he has been with the School of Information Engineering, Chang'an University, Xi'an, where he is currently a Professor. His research interests include ultra-wideband technology, wireless communication theory, the Internet of Things, and indoor positioning techniques.

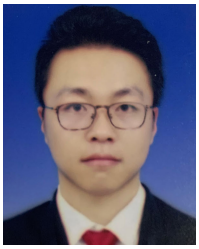

REN LIU was born in Qingyang, Gansu, China, in 1996. He is currently pursuing the Ph.D. degree with the Department of Communication Engineering, School of Information Engineering, Chang'an University. His research interest includes indoor visible light positioning techniques.

WEI LI (Member, IEEE) received the B.S. and M.S. degrees in electrical and electronics engineering from Xi'an Jiaotong University, China, in 2001 and 2004, respectively, and the Ph.D. degree from the Department of Information and Communication Engineering, Xi'an Jiaotong University, in 2016. From 2005 to 2011, he had been a Senior Engineer with Huawei Technology Corporation. From 2013 to 2015, he was a Visiting Student with the University of Maryland, College Park, USA. Since June 2016, he has become a Faculty Member of the School of Information Engineering, Chang'an University, China. His current research interests include green communications, energy harvesting, and cooperative communications in wireless networks. He serves and has served as a Technical Program Committee Member for some world-renowned conferences, including IEEE VTC and IEEE/CIC ICCC.